## Improving On-Demand Single Photon Source Coherence and Indistinguishability Through a Time-Delayed Coherent Feedback

Gavin Crowder, 1, 2, 3, \* Lora Ramunno, 1, 2 and Stephen Hughes<sup>3</sup>

<sup>1</sup>Department of Physics, University of Ottawa, Ottawa, Ontario, Canada, K1N 6N5
<sup>2</sup>Nexus for Quantum Technologies Institute, University of Ottawa, Ottawa, Ontario, Canada, K1N 6N5
<sup>3</sup>Department of Physics, Queen's University, Kingston, Ontario, Canada, K7L 3N6

Single photon sources (SPSs) form an essential resource for many quantum information technologies. We demonstrate how the inclusion of coherent feedback in a scalable waveguide system, can significantly improves the two key figures of merit: coherence and indistinguishability. Our feedback protocol is simulated using a quantum trajectory discretized waveguide model which can be used to directly model Hanbury Brown and Twiss (HBT) and Hong-Ou-Mandel (HOM) interferometers. With the proper choice of the round trip phase, the non-Markovian dynamics from the time-delayed feedback enhances the spontaneous emission rate and improves the coherence and indistinguishability of the SPS by up to 56%. We also show how this mechanism suppresses the effects of unwanted dissipation channels such as off-chip decay and pure dephasing.

The reliable generation of single photons is essential for the implementation of quantum information systems such as quantum cryptography or quantum computing [1]. Semiconductor quantum dots (QDs) have been shown to be an excellent source for generating quantum light in the form of single photons or photon pairs [2–13]. In particular, it has been shown that upon excitation by an appropriate laser pulse preparing the QD in the excited state, the QD can decay and emit a single photon into a desired output mode, e.g., a cavity or waveguide. This generation process is termed an "on-demand" due to (ideally) the production of a photon number state after each single laser pulse [14].

The key figures of merit associated with on-demand single photon sources (SPSs) are the efficiency,  $\eta$  (the probability of emitting a photon per laser pulse), the second order coherence,  $g^{(2)}(0)$  (related to the single photon purity), and the indistinguishability,  $\mathcal{I}$  (a measure of the coherence of the emitted photon state) [8, 15]. Significant research efforts have been developed to improve the efficiency, purity, and coherence of SPS generation. Indeed, state of the art systems have achieved  $g^{(2)}(0)=0.012$  and an indistinguishability of  $\mathcal{I}=0.962$  [9], though often these numbers are after filtering. Unwanted photon pair generation, out of plane emission, and dephasing events (such as through phonon absorption/emission [16, 17]) are all key challenges to overcome for continued improvement of these SPSs.

Feedback, where the output from a system is used as a stabilizing or control mechanism, has been well used across various platforms [18–28]. This is most often implemented through measurement-based feedback, where the output is measured to inform an external control which acts on the system [24–26, 29–33]. However, this approach is problematic for some quantum information systems that rely on maintaining system coherence as measurement of the output destroys coherence. Instead, the feedback can be included at the system level and act back on the system itself to avoid measurement: coherent

feedback. Recently, coherent feedback in waveguide quantum electrodynamic (QED) systems was shown to significantly alter the photon output statistics with continuous-wave pumping [18–23, 34–55]. Here, we will investigate if coherent feedback can be used in the *pulsed* laser regime to improve the figures of merit for a practical QD SPS.

Accurate simulation of coherent feedback is a difficult challenge in quantum circuits, since it introduces a non-Markovian dynamic. To calculate  $q^{(2)}(0)$  and  $\mathcal{I}$  requires knowledge of the two-time correlation functions, which typically use the quantum regression theorem (QRT) (although other specialized approaches have been developed, but they have their own practical limits [56, 57]). The QRT relies on a Markov approximation which fails in the presence of coherent feedback and other specialized techniques must be used [58–60]. A recently developed quantum trajectory discretized waveguide (QTDW) model which bypasses the non-Markovian dynamic by including the full feedback section of the waveguide at the system level. This is done through simulation of individual stochastic realizations of the system which give unique insights into the underlying stochastic system dynamics and can be averaged to obtain the ensemble dynamics. The model scales linearly with the number of photon states and is parallelizable which gives numerical advantages over density matrix techniques [53, 55].

In this Letter, we connect the QTDW model to photon correlation experiments, to compute  $g^{(2)}(0)$  and  $\mathcal{I}$  for waveguide-QED systems with coherent feedback, yielding direct simulations of Hanbury Brown and Twiss (HBT) or Hong-Ou-Mandel (HOM) interferometers. We summarize the key features of the QTDW model and outline its extension to simulate the HBT and HOM measurements. We then show how including a coherent feedback can significantly improve the  $g^{(2)}(0)$  and  $\mathcal{I}$  figures of merit for a QD SPS by up to 56%, and explain this improvement in the context of the feedback dynamics.

The system of interest, as shown in Fig. 1(a), is a single two-level system (TLS) coupled to a *truncated* waveguide

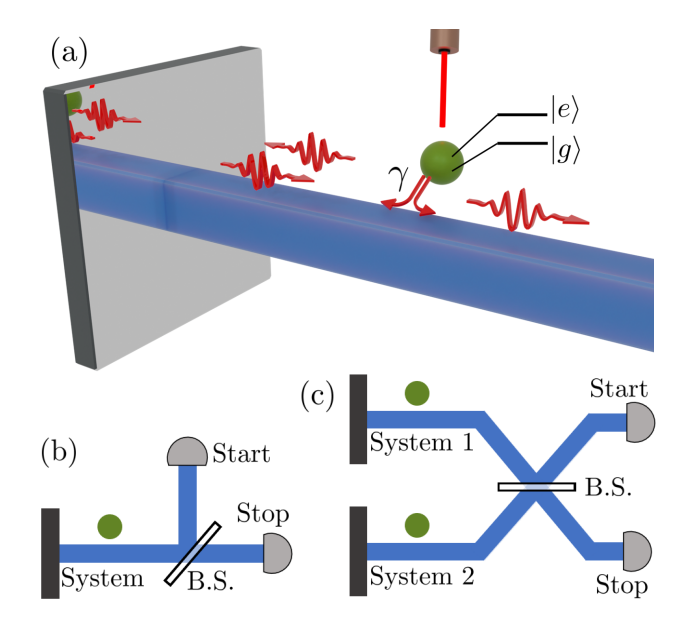


FIG. 1. Schematics of (a) the driven TLS setup with a coupled coherent feedback loop, (b) the HBT interferometer, and (c) the HOM interferometer; 'B.S.' represents a beam splitter.

which acts as a feedback loop, returning the output from the TLS to itself. An input laser pulse excites the TLS for single photon state emission. The total Hamiltonian in natural units ( $\hbar=1$ ) for the system, waveguide, and pump (in the interaction picture and with a rotating wave approximation) is  $H=H_{\rm W}+H_{\rm TLS}+H_{\rm I}+H_{\rm pump}$ . The TLS Hamiltonian is  $H_{\rm TLS}=\delta\sigma^+\sigma^-$  where  $\sigma^+$  ( $\sigma^-$ ) is the Pauli raising (lowering) operator and  $\delta=\omega_0-\omega_{\rm L}$  is the detuning between the TLS, with frequency  $\omega_0$ , and the laser, with frequency  $\omega_L$ . The pump Hamiltonian is  $H_{\rm pump}=\Omega(t)/2(\sigma^++\sigma^-)$  with the laser pulse shape given by  $\Omega(t)$  which drives the QD with a field orthogonal to the waveguide mode polarization [61–63].

In the continuous frequency domain, and in the interaction picture, the raising (lowering) operator for the photon modes in the waveguide are  $b^{\dagger}(\omega)$  ( $b(\omega)$ ) with Hamiltonian  $H_{\rm W} = \int_{-\infty}^{\infty} d\omega \, (\omega - \omega_{\rm L}) \, b^{\dagger}(\omega) b(\omega)$ , with  $[b(\omega), b^{\dagger}(\omega')] = \delta(\omega - \omega')$ . The interaction between the waveguide and TLS, with total radiative rate  $\gamma$  (and symmetric left and right coupling), is described by the Hamiltonian  $H_{\rm I} = \int_{-\infty}^{\infty} d\omega \, \left[ \left( \sqrt{\frac{\gamma}{4\pi}} \sigma^+ b(\omega) + \sqrt{\frac{\gamma}{4\pi}} e^{i(\phi_M + \omega \tau)} \sigma^+ b(\omega) \right) + {\rm H.c.} \right]$ , which incorporates the influence of the feedback loop, including the round trip delay time,  $\tau$ , and a mirror phase change,  $\phi_{\rm M}$ .

To model the feedback loop, we use a QTDW technique [53, 55], where the field operators for the waveguide section of interest (-L < x < 0) are transformed into the discrete time domain with operators  $B_n$ . These operators describe a unidirectional slice of the waveguide field which travels around the feedback loop, interacting twice with the TLS, located at the beginning and end of the loop. In this transformation,  $H_{\rm TLS}$  and  $H_{\rm pump}$  are

unchanged and the interaction Hamiltonian becomes

$$H_{\rm I} = \left(\sqrt{\frac{\gamma}{2\Delta t}}\sigma^{+}B_{N-1} + e^{i\phi}\sqrt{\frac{\gamma}{2\Delta t}}\sigma^{+}B_{0}\right) + \text{H.c.}, (1)$$

where  $\phi = \phi_{\rm M} + \omega_0 \tau$  is the round trip phase change and  $\Delta t = \tau/N$  is the time discretization of the feedback loop; now the TLS interacts with the incoming  $(N-1)^{\text{th}}$  bin  $(B_{N-1})$  and the outgoing zeroth bin  $(B_0)$  which picks up the phase change  $\phi$ . The key advantage of this approach appears in the evolution of the  $B_n$  operators under the waveguide Hamiltonian, which is  $U_{\rm W}^{\dagger}(\Delta t)B_nU_{\rm W}(\Delta t) =$  $e^{-i\delta\Delta t}B_{n-1}$ , where  $U_{\rm W}(\Delta t)=e^{-iH_{\rm W}\Delta t}$ . This evolution acts to pass the waveguide field forward one bin each time step, where we assume linear dispersion. The waveguide field outside of the loop, i.e., for x > 0, is modeled through the incoming and outgoing feedback loop bins, and the incoming bins are vacuum fields. During the QT step, we take a simulated measurement of the outgoing bin  $(B_0)$  and project the full ket vector accordingly. After projection, there is no information in the outgoing bin and it can be dropped to retain a tractable Hilbert space (absorbing boundary condition). This is a stochastic process, but an average over many individual QTs yields the ensemble average behavior of the system.

Importantly, a major advantage over other systemlevel quantum waveguide simulation approaches, is that we also include two important dissipation channels in our model of the TLS: (i) off chip decay from the TLS,  $C_0 = \sqrt{\gamma_0}\sigma^-$ , with rate  $\gamma_0$ , and (ii) pure dephasing in the TLS,  $C_1 = \sqrt{\gamma'}\sigma^+\sigma^-$ , with rate  $\gamma'$ . These are included as quantum jump operators following standard QT theory.

Using the QTDW model, we take advantage of the natural link between the individual QTs and experiments to calculate  $g^{(2)}(0)$  and  $\mathcal{I}$  through simulated HBT and HOM interferometers. Note that our technique can also tractably calculate the two-time correlation functions, however, the HBT and HOM approaches are more intuitive and numerically much faster.

In the HBT interferometer [15, 64], see Fig. 1(b), the output field  $a(t) = \langle B_0^{\dagger}(t)B_0(t)\rangle$ , is sent to a 50:50 beam-splitter and entangled with the vacuum field. The two output fields,  $c(t) = a(t)/\sqrt{2}$  and  $d(t) = a(t)/\sqrt{2}$ , are then measured by two detectors, a *start* detector and a *stop* detector. The detection times between the two detectors are correlated by taking the difference between the detection time on the *start* detector and all *stop* detection events, yielding a histogram of time-correlated detection records,  $h_{\text{HBT}}(t')$ . The system is driven by consecutive pulses separated by a delay time, T, long enough for the system to completely relax into the ground state.

To simulate the HBT detection, to take advantage of the parallelization of the QT technique, we run each QT independently with a single pulse coming in to drive the system and then allowing it to relax for a total run time of T. Next, we place these QTs in sequential order so that each pulse is separated by T and treat it as one long single QT. Since the beam-splitter equally splits the output field, to get the time-correlated detection records we stochastically assign each output jump event in the trajectory to either the start or stop detector and then correlate the two detection records to build the histogram,  $h_{\rm HBT}(t')$ , where  $\tau$  is the time difference between start and stop events. Assuming no correlations between pulses, when T is chosen sufficiently large, then

$$g^{(2)}(0) = \frac{A_{\text{HBT}}(0)}{A_{\text{HBT}}(T)} \left( 1 \pm \sqrt{\frac{1}{A_{\text{HBT}}(0)} + \frac{1}{A_{\text{HBT}}(T)}} \right), \tag{2}$$

with  $A_{\rm HBT}(0)$  the area of the peak centered at 0 and  $A_{\rm HBT}(T)$  the area of the next peak, centered at T. A sufficiently large number of trajectories is carried out to approach an accurate average.

In the HOM simulation [15, 65], see Fig. 1(c), we take the interference between the output of two independent copies ('1' or '2') of our system incident on a 50:50 beam splitter (which can easily be extended to an unequal beam splitter). The output from system-1 is  $a(t) = \langle B_0^{\dagger(1)}(t)B_0^{(1)}(t)\rangle$  and the output from system-2 is  $b(t) = \langle B_0^{\dagger(2)}(t)B_0^{(2)}(t)\rangle$ . These fields are entangled on the beam splitter and the resulting fields are  $c'(t) = (a(t)+b(t))/\sqrt{2}$  and  $d'(t) = (a(t)-b(t))/\sqrt{2}$ . We again drive both copies with consecutive pulses of delay time, T, and time-correlate the detection records of a start and stop detector which measure the c'(t) and d'(t) fields, respectively. Similar to the HBT interferometer, the correlated detection record can be used to yield a histogram,  $h_{\text{HOM}}(t')$ .

This HOM setup is more difficult to simulate with the QT technique compared to the HBT interferometer, as the detection records for c'(t) and d'(t) are no longer accessible through our jump record of  $B_0$ . Instead we entangle two copies of our system using a tensor product, so that the total Hamiltonian is  $H_{\text{HOM}} = H^{(1)} \otimes H^{(2)}$ , since the two systems are completely independent to begin with. Then, rather than taking our output operators to be  $B_0^{(1)}$  and  $B_0^{(2)}$ , we use the entangled fields after the beam-splitter:

$$B_{\text{start}} = \frac{B_0^{(1)} + B_0^{(2)}}{\sqrt{2}}, \ B_{\text{stop}} = \frac{B_0^{(1)} - B_0^{(2)}}{\sqrt{2}}.$$
 (3)

Next, when we detect a photon in the *start* (*stop*) detector, we apply the operator  $B_{\text{start}}$  ( $B_{\text{stop}}$ ) to the combined system. Detection times are recorded to build up detection records for the two detectors which we can time-correlate. From  $h_{\text{HOM}}(t')$ ,

$$g_{\text{HOM}}^{(2)}(0) = \frac{A_{\text{HOM}}(0)}{A_{\text{HOM}}(T)} \left( 1 \pm \sqrt{\frac{1}{A_{\text{HOM}}(0)} + \frac{1}{A_{\text{HOM}}(T)}} \right), \tag{4}$$

which is related to the indistinguishability through [8, 15]

$$\mathcal{I} = 1 - g_{\text{HOM}}^{(2)}(0). \tag{5}$$

Without feedback, i.e., for a TLS coupled to an open waveguide [6, 8, 62, 66], to generate a SPS we pump the system with a  $\pi$ -pulse to excite the TLS and decay back to the ground state, emitting a single photon. In the limit of an infinitely short pulse width, and neglecting phonon interactions [8], or any other decoherence operators in the system, this TLS is considered to be a perfect SPS with  $g^{(2)}(0) = 0$  and  $\mathcal{I} = 1$ . The perfection of these sources fail when a finite pulse width is taken to account (as this introduces a chance of two photon emission from the system) and sources of detuning and off-chip decay are included (which spoils the coherence) [67].

With a strategic choice of  $\phi$ , coherent feedback has been shown to enhance the spontaneous emission rate of the system. We harness this aspect of feedback to improve the TLS as a SPS. The TLS is driven by a Gaussian  $\pi$ -pulse, defined by  $\Omega(t) = \left(\pi/\sigma\sqrt{2\pi}\right) \exp\left[-t^2/2\sigma^2\right]$ , where  $\sigma = t_p/2\sqrt{2\ln 2}$  and  $t_p$  is the FWHM pulse width.

Figure 2 demonstrates that significant improvements in both the second order coherence and indistinguishability are obtained when coherent feedback is included. We show results with and without feedback (orange and blue lines, respectively) as a function of changing pulse width, off chip decay rate, and pure dephasing rate. Note the error is not shown because the number of trajectories run for each data point result in negligible uncertainty. Our ranges cover typical experimental values with QD waveguide systems [63, 68, 69]. In Figs. 2(a) and (b), the second order coherence is improved by including feedback at all pulse widths, both with (Fig 2(b)) and without (Fig. 2(a)) the additional Lindblad output channels. The inclusion of dephasing and off-chip decay do not have a significant impact on  $g^{(2)}(0)$  and the majority of the improvement by including feedback is a result of suppressing the two-photon emission probability that arises from the finite pulse width. Across all pulse widths we find an average relative improvement in the coherence of 56%.

Next, the indistinguishability versus incoming pulse width is shown in Figs. 2(e) and (f), and again we find that coherent feedback significantly improves the output at all pulse widths. The indistinguishability is dependent on maintaining the coherence of the system throughout the decay time of the TLS so when detuning is included these is a large reduction to  $\mathcal{I}$ . By increasing the spontaneous emission rate, feedback reduces the decay time of the TLS and there is less opportunity for a dephasing event to occur. Without pure dephasing we see an average relative improvement in the indistinguishability of 55% and with pure dephasing the average relative improvement is 40%.

Figure 3 shows an example histogram that is constructed from the HOM simulation and used to calculate  $\mathcal{I}$ . The chosen pulse width was  $\gamma t_p = 0.01$  and both

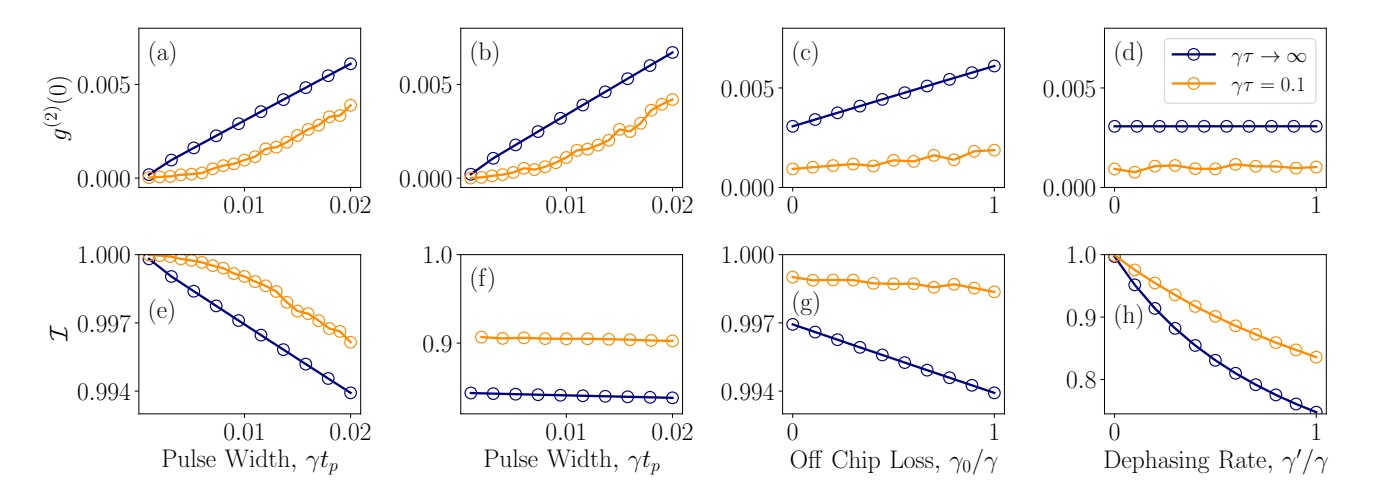


FIG. 2. (a)-(d) The second order coherence and (e)-(h) the indistinguishability of the output single photons. The width of the incoming pulse is varied without additional dissipation channels  $C_0$  and  $C_1$  in (a) and (e), while these channels are included ( $\gamma_0 = 0.1\gamma$  and  $\gamma' = 0.5\gamma$ ) in (b) and (f). The pulse width is then set at  $\gamma t_p = 0.01$  and the off chip decay rate is varied in (c) and (g) with  $\gamma' = 0$ , while the pure dephasing rate is varied in (d) and (h) with  $\gamma_0 = 0$ . Each data point with feedback is an average of 500,000 trajectories.

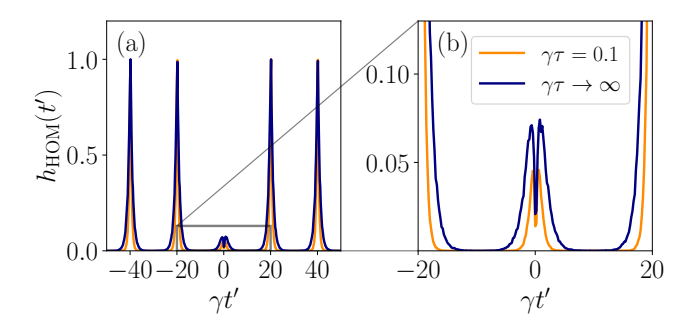


FIG. 3. (a) Sample histograms from a simulation of the HOM interferometer with feedback and without feedback, along with (b) a zoom in on the center peak. A pulse width of  $\gamma t_p = 0.01$  was chosen and additional dissipation channels were included with rates  $\gamma' = 0.5\gamma$  and  $\gamma_0 = 0.1\gamma$ . Each histogram is an average of 500,000 trajectories.

Lindblad operators were included with rates  $\gamma_0 = 0.1\gamma$  and  $\gamma' = 0.5\gamma$ . Each data point in the histogram shows the number of events with a delay time of  $\gamma t'$  between the 'start' and 'stop' detections of the HOM interferometer setup. Since each pulse is separated by a delay, T (in this case  $\gamma T = 20$ ), the central peak at  $\gamma t' = 0$  is the result of both a start and stop detection occurring within a single pulse cycle. If both systems maintain coherence, then the two emitted photons in the entangled field will be observed through the same detector. Thus, each count that appears in the central peak is a simulation where the coherence between the two systems copies is lost, whether that is from a pure dephasing, off-chip decay, or two-photon emission event.

Each peak is centered around the arrival time of the pump pulses, and the width of the peak is determined

by the delay between the excitation and the emission. Comparing the two histograms, the peaks with feedback are much sharper than without. This is because the enhanced spontaneous emission with feedback decreases the delay between excitation and emission which in turn decreases the variance in emission times after each pulse, sharpening each peak. Also, since the emission delay is shortened there is less time for any of the undesirable decoherence events (in particular a dephasing blip) to occur. This decreases the area of the central peak and leads to an increase in the indistinguishability with feedback.

We also compare  $g^{(2)}(0)$  and  $\mathcal{I}$  with and without feedback as a function of the off-chip decay rate in Figs. 2(c) and (g), and as a function of the pure dephasing rate in Figs. 2(d) and (h), with a fixed pulse width. Note that the improvement at  $\gamma_0 = \gamma' = 0$  is purely due to the improvement from two-photon emission suppression that is seen in Fig. 2(a). Instead we are interested in how well feedback suppresses the penalty to  $q^{(2)}(0)$  or  $\mathcal{I}$  from including off-chip decay or pure dephasing. We find that for off-chip decay (Figs. 2(c) and (g)), feedback does an excellent job of suppressing the effects of the additional output channel, decreasing the impact on coherence by 70% and on indistinguishability by 82%. For the pure dephasing rate (Figs. 2(d) and (h)),  $g^{(2)}(0)$ is not affected by the increase in pure dephasing events so there is little difference between the results with and without feedback. Pure dephasing has its greatest affect on the indistinguishability, and feedback does a good job of reducing its impact, suppressing its effects by 39%.

In summary, we have exploited a QTDW model to calculate the  $g^{(2)}(0)$  and  $\mathcal I$  figures of merit for a SPS by directly simulating an HBT or HOM interferometer. This approach allows one to bypass the quantum regression

theorem in order to simulate the non-Markovian dynamics that arise when coherent feedback is included in a waveguide-QED system. Using this technique, we have shown that direct inclusion of coherent feedback can improve the coherence and indistinguishability of a SPS, even when pure dephasing is a significant source of decoherence in the system. This work only harnesses a single characteristic of feedback, namely its ability to enhance spontaneous emission, in order to achieve these improvements. In future work, other aspects of feedback such as excitation trapping and additional nonlinear behavior might be useful for photon pair emission and other quantum information system objectives.

This work was supported by the Natural Sciences and Engineering Research Council of Canada (NSERC), the National Research Council of Canada (NRC), Queen's University, and the University of Ottawa. We thank Dan Dalacu and Robin Williams for support and useful discussions.

## \* gcrow088@uottawa.ca

- A. Kiraz, M. Atatüre, and A. Imamoğlu, Quantum-dot single-photon sources: Prospects for applications in linear optics quantum-information processing, Physical Review A 69, 032305 (2004).
- [2] C. Santori, D. Fattal, J. Vučković, G. S. Solomon, E. Waks, and Y. Yamamoto, Submicrosecond correlations in photoluminescence from InAs quantum dots, Physical Review B 69, 205324 (2004).
- [3] K. Takemoto, Y. Sakuma, S. Hirose, T. Usuki, N. Yokoyama, T. Miyazawa, M. Takatsu, and Y. Arakawa, Non-classical Photon Emission from a Single InAs/InP Quantum Dot in the 1.3-µm Optical-Fiber Band, Japanese Journal of Applied Physics 43, L993 (2004).
- [4] G. Cui and M. G. Raymer, Emission spectra and quantum efficiency of single-photon sources in the cavity-QED strong-coupling regime, Physical Review A 73, 053807 (2006).
- [5] Y.-M. He, Y. He, Y.-J. Wei, D. Wu, M. Atatüre, C. Schneider, S. Höfling, M. Kamp, C.-Y. Lu, and J.-W. Pan, On-demand semiconductor single-photon source with near-unity indistinguishability, Nature Nanotechnology 8, 213 (2013).
- [6] S. Kalliakos, Y. Brody, A. Schwagmann, A. J. Bennett, M. B. Ward, D. J. P. Ellis, J. Skiba-Szymanska, I. Farrer, J. P. Griffiths, G. A. C. Jones, D. A. Ritchie, and A. J. Shields, In-plane emission of indistinguishable photons generated by an integrated quantum emitter, Applied Physics Letters 104, 221109 (2014), publisher: American Institute of Physics.
- [7] M. Paul, J. Kettler, K. Zeuner, C. Clausen, M. Jetter, and P. Michler, Metal-organic vapor-phase epitaxy-grown ultra-low density InGaAs/GaAs quantum dots exhibiting cascaded single-photon emission at 1.3  $\mu$ m, Applied Physics Letters 106, 122105 (2015).

- [8] S. Hughes, S. Franke, C. Gustin, M. Kamandar Dezfouli, A. Knorr, and M. Richter, Theory and Limits of On-Demand Single-Photon Sources Using Plasmonic Resonators: A Quantized Quasinormal Mode Approach, ACS Photonics 6, 2168 (2019).
- [9] Y.-M. He, H. Wang, C. Wang, M.-C. Chen, X. Ding, J. Qin, Z.-C. Duan, S. Chen, J.-P. Li, R.-Z. Liu, C. Schneider, M. Atatüre, S. Höfling, C.-Y. Lu, and J.-W. Pan, Coherently driving a single quantum two-level system with dichromatic laser pulses, Nature Physics 15, 941 (2019).
- [10] P. Laferrière, E. Yeung, I. Miron, D. B. Northeast, S. Haffouz, J. Lapointe, M. Korkusinski, P. J. Poole, R. L. Williams, and D. Dalacu, Unity yield of deterministically positioned quantum dot single photon sources, Scientific Reports 12, 6376 (2022).
- [11] M. H. Appel, A. Tiranov, S. Pabst, M. L. Chan, C. Starup, Y. Wang, L. Midolo, K. Tiurev, S. Scholz, A. D. Wieck, A. Ludwig, A. S. Sørensen, and P. Lodahl, Entangling a Hole Spin with a Time-Bin Photon: A Waveguide Approach for Quantum Dot Sources of Multiphoton Entanglement, Physical Review Letters 128, 233602 (2022).
- [12] L. Ginés, M. Moczała-Dusanowska, D. Dlaka, R. Hošák, J. R. Gonzales-Ureta, J. Lee, M. Ježek, E. Harbord, R. Oulton, S. Höfling, A. B. Young, C. Schneider, and A. Predojević, High Extraction Efficiency Source of Photon Pairs Based on a Quantum Dot Embedded in a Broadband Micropillar Cavity, Physical Review Letters 129, 033601 (2022).
- [13] B. Da Lio, C. Faurby, X. Zhou, M. L. Chan, R. Uppu, H. Thyrrestrup, S. Scholz, A. D. Wieck, A. Ludwig, P. Lodahl, and L. Midolo, A Pure and Indistinguishable Single-Photon Source at Telecommunication Wavelength, Advanced Quantum Technologies 5, 2200006 (2022).
- [14] T. K. Bracht, M. Cosacchi, T. Seidelmann, M. Cygorek, A. Vagov, V. M. Axt, T. Heindel, and D. E. Reiter, Swing-Up of Quantum Emitter Population Using Detuned Pulses, PRX Quantum 2, 040354 (2021).
- [15] K. A. Fischer, K. Müller, K. G. Lagoudakis, and J. Vučković, Dynamical modeling of pulsed two-photon interference, New Journal of Physics 18, 113053 (2016).
- [16] J. Iles-Smith, D. P. S. McCutcheon, A. Nazir, and J. Mørk, Phonon scattering inhibits simultaneous nearunity efficiency and indistinguishability in semiconductor single-photon sources, Nature Photonics 11, 521 (2017).
- [17] C. Gustin and S. Hughes, Pulsed excitation dynamics in quantum-dot-cavity systems: Limits to optimizing the fidelity of on-demand single-photon sources, Phys. Rev. B 98, 045309 (2018).
- [18] U. Dorner and P. Zoller, Laser-driven atoms in halfcavities, Physical Review A 66, 023816 (2002).
- [19] T. Tufarelli, F. Ciccarello, and M. S. Kim, Dynamics of spontaneous emission in a single-end photonic waveguide, Physical Review A 87, 013820 (2013).
- [20] A. Carmele, J. Kabuss, F. Schulze, S. Reitzenstein, and A. Knorr, Single Photon Delayed Feedback: A Way to Stabilize Intrinsic Quantum Cavity Electrodynamics, Physical Review Letters 110, 013601 (2013).
- [21] N. L. Naumann, L. Droenner, S. M. Hein, A. Carmele, A. Knorr, and J. Kabuss, Feedback control of optomechanical systems, in *Physics and Simulation of Optoelectronic Devices XXIV*, Vol. 9742 (International Society for Optics and Photonics, 2016) p. 974216.

- [22] Y. Lu, N. L. Naumann, J. Cerrillo, Q. Zhao, A. Knorr, and A. Carmele, Intensified antibunching via feedbackinduced quantum interference, Physical Review A 95, 063840 (2017).
- [23] H. Pichler, S. Choi, P. Zoller, and M. D. Lukin, Universal photonic quantum computation via time-delayed feedback, Proceedings of the National Academy of Sciences 114, 11362 (2017).
- [24] H. M. Wiseman and G. J. Milburn, Quantum Measurement and Control (Cambridge University Press, Oxford, 2002) p. 231.
- [25] M. H. Muñoz Arias, I. H. Deutsch, P. S. Jessen, and P. M. Poggi, Simulation of complex dynamics of mean-field p-spin models using measurement-based quantum feedback control, Physical Review A 102, 022610 (2020).
- [26] T. Grigoletto and F. Ticozzi, Stabilization Via Feedback Switching for Quantum Stochastic Dynamics, IEEE Control Systems Letters 6, 235 (2021).
- [27] D. R. Hjelme, A. R. Mickelson, and R. G. Beausoleil, Semiconductor laser stabilization by external optical feedback, IEEE Journal of Quantum Electronics 27, 352 (1991).
- [28] G. F. Franklin, J. D. Powell, and A. Emami-Naeini, Feed-back Control of Dynamic Systems (Pearson, 2014).
- [29] A. Kubanek, M. Koch, C. Sames, A. Ourjoumtsev, P. W. H. Pinkse, K. Murr, and G. Rempe, Photon-byphoton feedback control of a single-atom trajectory, Nature 462, 898 (2009).
- [30] G. G. Gillett, R. B. Dalton, B. P. Lanyon, M. P. Almeida, M. Barbieri, G. J. Pryde, J. L. O'Brien, K. J. Resch, S. D. Bartlett, and A. G. White, Experimental feedback control of quantum systems using weak measurements, Phys. Rev. Lett. 104, 080503 (2010).
- [31] M. Rafiee, A. Nourmandipour, and S. Mancini, Enforcing dissipative entanglement by feedback, Physics Letters A 384, 126748 (2020).
- [32] Z. Tan, P. A. Camati, G. C. Cauquil, A. Auffèves, and I. Dotsenko, Alternative experimental ways to access entropy production, Phys. Rev. Research 3, 043076 (2021).
- [33] A. Di Giovanni, M. Brunelli, and M. G. Genoni, Unconditional mechanical squeezing via backaction-evading measurements and nonoptimal feedback control, Physical Review A 103, 022614 (2021).
- [34] K. Koshino and Y. Nakamura, Control of the radiative level shift and linewidth of a superconducting artificial atom through a variable boundary condition, New Journal of Physics 14, 043005 (2012).
- [35] I.-C. Hoi, A. F. Kockum, L. Tornberg, A. Pourkabirian, G. Johansson, P. Delsing, and C. M. Wilson, Probing the quantum vacuum with an artificial atom in front of a mirror, Nature Physics 11, 1045 (2015).
- [36] A. L. Grimsmo, Time-Delayed Quantum Feedback Control, Physical Review Letters 115, 060402 (2015).
- [37] J. Kabuss, F. Katsch, A. Knorr, and A. Carmele, Unraveling coherent quantum feedback for Pyragas control, Journal of the Optical Society of America B 33, C10 (2016).
- [38] H. Pichler and P. Zoller, Photonic Circuits with Time Delays and Quantum Feedback, Physical Review Letters 116, 093601 (2016).
- [39] N. Német and S. Parkins, Enhanced optical squeezing from a degenerate parametric amplifier via time-delayed coherent feedback, Physical Review A 94, 023809 (2016).
- [40] S. M. Hein, A. Carmele, and A. Knorr, Creation and con-

- trol of entanglement by time-delayed quantum-coherent feedback, in *Physics and Simulation of Optoelectronic Devices XXIV*, Vol. 9742 (International Society for Optics and Photonics, 2016) p. 97420X.
- [41] P.-O. Guimond, H. Pichler, A. Rauschenbeutel, and P. Zoller, Chiral quantum optics with V-level atoms and coherent quantum feedback, Physical Review A 94, 033829 (2016).
- [42] S. J. Whalen, A. L. Grimsmo, and H. J. Carmichael, Open quantum systems with delayed coherent feedback, Quantum Science and Technology 2, 044008 (2017).
- [43] N. L. Naumann, S. M. Hein, M. Kraft, A. Knorr, and A. Carmele, Feedback control of photon statistics, in *Physics and Simulation of Optoelectronic Devices XXV*, Vol. 10098 (International Society for Optics and Photonics, 2017) p. 100980N.
- [44] P.-O. Guimond, M. Pletyukhov, H. Pichler, and P. Zoller, Delayed coherent quantum feedback from a scattering theory and a matrix product state perspective, Quantum Science and Technology 2, 044012 (2017).
- [45] P. Forn-Díaz, C. Warren, C. Chang, A. Vadiraj, and C. Wilson, On-Demand Microwave Generator of Shaped Single Photons, Physical Review Applied 8, 054015 (2017).
- [46] S. J. Whalen, Collision model for non-Markovian quantum trajectories, Physical Review A 100, 052113 (2019).
- [47] N. Német, S. Parkins, A. Knorr, and A. Carmele, Stabilizing quantum coherence against pure dephasing in the presence of time-delayed coherent feedback at finite temperature, Physical Review A 99, 053809 (2019).
- [48] G. Calajó, Y.-L. L. Fang, H. U. Baranger, and F. Ciccarello, Exciting a Bound State in the Continuum through Multiphoton Scattering Plus Delayed Quantum Feedback, Physical Review Letters 122, 073601 (2019).
- [49] G. Crowder, H. Carmichael, and S. Hughes, Quantum trajectory theory of few-photon cavity-QED systems with a time-delayed coherent feedback, Physical Review A 101, 023807 (2020).
- [50] A. Harwood, M. Brunelli, and A. Serafini, Cavity optomechanics assisted by optical coherent feedback, Physical Review A 103, 023509 (2021).
- [51] K. Barkemeyer, M. Hohn, S. Reitzenstein, and A. Carmele, Boosting energy-time entanglement using coherent time-delayed feedback, Physical Review A 103, 062423 (2021).
- [52] Y. Shi and E. Waks, Deterministic generation of multidimensional photonic cluster states using time-delay feedback, Physical Review A 104, 013703 (2021).
- [53] S. Arranz Regidor, G. Crowder, H. Carmichael, and S. Hughes, Modeling quantum light-matter interactions in waveguide QED with retardation, nonlinear interactions, and a time-delayed feedback: Matrix product states versus a space-discretized waveguide model, Physical Review Research 3, 023030 (2021).
- [54] K. Barkemeyer, A. Knorr, and A. Carmele, Heisenberg treatment of multiphoton pulses in waveguide QED with time-delayed feedback, Physical Review A 106, 023708 (2022).
- [55] G. Crowder, L. Ramunno, and S. Hughes, Quantum trajectory theory and simulations of nonlinear spectra and multiphoton effects in waveguide-QED systems with a time-delayed coherent feedback, Physical Review A 106, 013714 (2022).
- [56] M. Cosacchi, T. Seidelmann, M. Cygorek, A. Vagov,

- D. Reiter, and V. Axt, Accuracy of the Quantum Regression Theorem for Photon Emission from a Quantum Dot, Physical Review Letters 127, 100402 (2021).
- [57] M. Richter and S. Hughes, Enhanced TEMPO Algorithm for Quantum Path Integrals with Off-Diagonal System-Bath Coupling: Applications to Photonic Quantum Networks, Physical Review Letters 128, 167403 (2022).
- [58] C. Gardiner and P. Zoller, Quantum Noise: A Handbook of Markovian and Non-Markovian Quantum Stochastic Methods with Applications to Quantum Optics (Springer-Verlag, Berlin, 2000).
- [59] P. Stenius and A. Imamoglu, Stochastic wavefunction methods beyond the Born - Markov and rotatingwave approximations, Quantum and Semiclassical Optics: Journal of the European Optical Society Part B 8, 283 (1996).
- [60] D. Chruściński and A. Kossakowski, Non-Markovian Quantum Dynamics: Local versus Nonlocal, Physical Review Letters 104, 070406 (2010).
- [61] M. N. Makhonin, J. E. Dixon, R. J. Coles, B. Royall, I. J. Luxmoore, E. Clarke, M. Hugues, M. S. Skolnick, and A. M. Fox, Waveguide Coupled Resonance Fluorescence from On-Chip Quantum Emitter, Nano Letters 14, 6997 (2014).
- [62] R. Uppu, F. T. Pedersen, Y. Wang, C. T. Olesen, C. Papon, X. Zhou, L. Midolo, S. Scholz, A. D. Wieck, A. Ludwig, and P. Lodahl, Scalable integrated single-photon source, Science Advances 6, eabc8268 (2020).
- [63] L. Dusanowski, C. Gustin, S. Hughes, C. Schneider, and

- S. Höfling, All-Optical Tuning of Indistinguishable Single Photons Generated in Three-Level Quantum Systems, Nano Letters **22**, 3562 (2022).
- [64] R. H. Brown and R. Q. Twiss, Correlation between Photons in two Coherent Beams of Light, Nature 177, 27 (1956).
- [65] C. K. Hong, Z. Y. Ou, and L. Mandel, Measurement of subpicosecond time intervals between two photons by interference, Physical Review Letters 59, 2044 (1987).
- [66] P. Schnauber, A. Singh, J. Schall, S. I. Park, J. D. Song, S. Rodt, K. Srinivasan, S. Reitzenstein, and M. Davanco, Indistinguishable Photons from Deterministically Integrated Single Quantum Dots in Heterogeneous GaAs/Si3N4 Quantum Photonic Circuits, Nano Letters 19, 7164 (2019).
- [67] C. Gustin, R. Manson, and S. Hughes, Spectral asymmetries in the resonance fluorescence of two-level systems under pulsed excitation, Optics Letters 43, 779 (2018).
- [68] K. Mnaymneh, D. Dalacu, J. McKee, J. Lapointe, S. Haffouz, J. F. Weber, D. B. Northeast, P. J. Poole, G. C. Aers, and R. L. Williams, On-chip integration of single photon sources via evanescent coupling of tapered nanowires to SiN waveguides, Advanced Quantum Technologies 3, 1900021 (2019).
- [69] P. Türschmann, H. L. Jeannic, S. F. Simonsen, H. R. Haakh, S. Götzinger, V. Sandoghdar, P. Lodahl, and N. Rotenberg, Coherent nonlinear optics of quantum emitters in nanophotonic waveguides, Nanophotonics 8, 1641 (2019).